

# Double-quarkonium production at a fixed-target experiment at the LHC (AFTER@LHC)

Jean-Philippe Lansberg<sup>a</sup>, Hua-Sheng Shao<sup>b</sup>

<sup>a</sup>IPNO, Université Paris-Sud, CNRS/IN2P3, F-91406, Orsay, France

<sup>b</sup>PH Department, TH Unit, CERN, CH-1211, Geneva 23, Switzerland

---

## Abstract

We present predictions for double-quarkonium production in the kinematical region relevant for the proposed fixed-target experiment using the LHC beams (dubbed as AFTER@LHC). These include all spin-triplet  $S$ -wave charmonium and bottomonium pairs, i.e.  $\psi(n_1S) + \psi(n_2S)$ ,  $\psi(n_1S) + \Upsilon(m_1S)$  and  $\Upsilon(m_1S) + \Upsilon(m_2S)$  with  $n_1, n_2 = 1, 2$  and  $m_1, m_2 = 1, 2, 3$ . We calculate the contributions from double-parton scatterings and single-parton scatterings. With an integrated luminosity of  $20 \text{ fb}^{-1}$  to be collected at AFTER@LHC, we find that the yields for double-charmonium production are large enough for differential distribution measurements. We discuss some differential distributions for  $J/\psi + J/\psi$  production, which can help to study the physics of double-parton and single-parton scatterings in a new energy range and which might also be sensitive to double intrinsic  $c\bar{c}$  coalescence at large negative Feynman  $x$ .

*Keywords:* Quarkonium production

*PACS:* 12.38.Bx, 14.40.Gx, 13.85.Ni

---

## 1. Introduction

Heavy-quarkonium production is typically a multi-scale process, which involves both short- and long-distance aspects of the strong interaction. This particularity makes heavy-quarkonium production an ideal probe to study Quantum Chromodynamics (QCD) in its perturbative and non-perturbative regimes simultaneously. Studies have extensively been performed at collider and fixed-target energies in proton-proton, proton-nucleus and nucleus-nucleus collisions (see reviews e.g. Refs. [1, 2, 3]). The associated production of heavy quarkonium is a very interesting process not only because it provides a way to pin down the heavy-quarkonium production mechanism but also because it can help to understand a new dynamics of hadron collisions appearing at high energies, where multiple-parton scatterings (MPS) happen simultaneously, among which the most likely is of course two short-distance interactions from a single hadron-hadron collision – double-parton scattering (DPS). The relevant DPS analyses with heavy quarkonium are  $J/\psi + W$  [4],  $J/\psi + Z$  [5],  $J/\psi + \text{charm}$  [6] and  $J/\psi + J/\psi$  [7] production.

In particular, double-quarkonium production is of specific interest. It provides an original tool to study quarkonium production from the conventional single-parton scatterings (SPSs). The

relevant earlier studies in the literature can be found in Refs. [8, 9, 10, 11, 12, 13, 14, 15, 16, 17, 18, 19]. Moreover, it was claimed in Refs. [20, 21, 22, 23, 24, 25, 18, 19] that DPS contributions should be significant source of  $J/\psi + J/\psi$ , especially at high energies where there is a high parton flux. In addition, the spin-triplet  $S$ -waves (*e.g.*  $J/\psi$ ,  $\Upsilon$ ) provide clean signatures with their small background when they are studied in their decay into muon pairs. Hence, they are easy to trigger on experimentally, in contrast to hadronic jets and open charm mesons productions, which require either good calorimetry or good particle identification.

A first comprehensive comparison between experiments [26, 7, 27] and theory for  $J/\psi$ -pair production at the Tevatron and the LHC was performed in Ref. [18], where we pointed out that this observable could be used to probe different mechanisms in different kinematical regions. We noted that the direct DPS measurement by D0 collaboration [7] –looking at the rapidity-difference spectrum– is consistent with the  $J/\psi$ -pair measurement by the CMS collaboration [27] and, as we will discuss later on, compatible with rather larger DPS rates. On the other hand, as we advocated in [16], one cannot draw a definite conclusion on the presence of DPS in the LHCb data [26] with relatively low statistics.

In this context, we found it important to study the potentialities offered by the use of the 7 TeV proton LHC beams used in the fixed target mode to study quarkonium pair production. Its multi-TeV beams indeed allow one to study  $p + p$ ,  $p + d$  and  $p + A$  collisions at a centre-of-mass energy  $\sqrt{s_{NN}} \simeq 115$  GeV as well as  $Pb + p$  and  $Pb + A$  collisions at  $\sqrt{s_{NN}} \simeq 72$  GeV, with the high precision typical of the fixed-target mode. It was indeed advocated in [3, 28] that such a facility, referred to as AFTER@LHC, would become a quarkonium, prompt photon and heavy-flavour observatory thanks to its large expected luminosity (for recent phenomenological studies, see [29, 30, 31, 32, 33, 34, 35, 36, 37, 38]). A first feasibility study for quarkonium production was presented in [39] and demonstrated that a LHCb-like detector would perform extremely well in the fixed-target mode. Similar performances are expected for quarkonium-pair production.

Integrated luminosities as large as  $20 \text{ fb}^{-1}$  [3] can be delivered during a one-year run of  $p + H$  collisions with a bent crystal to extract the beam [40]. The LHC beam can also go through an internal-gas-target system<sup>1</sup>. Conservatively sticking to gas pressures already reachable now, yearly integrated luminosities reach  $100 \text{ pb}^{-1}$ . With a designed target cell similar to that of HERMES [44], a few  $\text{fb}^{-1} \text{ yr}^{-1}$  are probably also reachable. We have reported in Tab. 1 the instantaneous and yearly integrated luminosities expected with the proton beams on various target species of various thicknesses, for both options.

The structure of this paper is as follows. In section 2, we detail and justify our methodology to compute both DPS and SPS contributions to quarkonium-pair production. Section 3 contains a general discussion of the interest to look at DPS vs SPS contributions at different energies. This prepares the discussion of our results at  $\sqrt{s} = 115$  GeV relevant for AFTER@LHC in Section 4. Section 5 gathers our conclusions.

---

<sup>1</sup>This is in fact already tested at low gas pressures by the LHCb collaboration in order to monitor the luminosity of the beam [41, 42, 43].

Beam	Target	Thickness (cm)	$\rho$ (g.cm <sup>-3</sup> )	$\mathcal{L}$ ( $\mu\text{b}^{-1}.\text{s}^{-1}$ )	$\int \mathcal{L}$ ( $\text{pb}^{-1}.\text{y}^{-1}$ )
p	Liquid H	100	0.068	2000	20000
Beam	Target	Usable gas zone (cm)	Pressure (Bar)	$\mathcal{L}$ ( $\mu\text{b}^{-1}.\text{s}^{-1}$ )	$\int \mathcal{L}$ ( $\text{pb}^{-1}.\text{y}^{-1}$ )
p	perfect gas	100	10 <sup>-9</sup>	10	100

Table 1: Expected luminosities obtained for a 7 TeV proton beam extracted by means of a bent crystal or obtained with an internal gas target with a pressure similar to that of SMOG@LHCb [42].

## 2. Methodology

In this section, we will explain the main ingredients used to compute the rates of double-quarkonium production at AFTER@LHC, which closely follows from our previous work in Ref. [18].

### 2.1. Double-parton scatterings

The description of such a mechanism is usually done by assuming that DPS can be factorised into two single-parton scatterings (SPS); this can be seen as a first rough approximation which can however be justified by the fact that possible unfactorisable corrections due to parton correlations should be small at small  $x$ . For the double-quarkonium production, the general formalism with a factorisation assumption is (see e.g. Ref. [24])

$$\sigma_{Q_1 Q_2} = \frac{1}{1 + \delta_{Q_1 Q_2}} \sum_{i,j,k,l} \int dx_1 dx_2 dx'_1 dx'_2 d^2 \mathbf{b}_1 d^2 \mathbf{b}_2 d^2 \mathbf{b} \times \Gamma_{ij}(x_1, x_2, \mathbf{b}_1, \mathbf{b}_2) \hat{\sigma}_{ik}^{Q_1}(x_1, x'_1) \hat{\sigma}_{jl}^{Q_2}(x_2, x'_2) \Gamma_{kl}(x'_1, x'_2, \mathbf{b}_1 - \mathbf{b}, \mathbf{b}_2 - \mathbf{b}), \quad (1)$$

where  $\delta_{Q_1 Q_2}$  is the Kronecker delta function,  $\Gamma_{ij}(x_1, x_2, \mathbf{b}_1, \mathbf{b}_2)$  is the generalised double distributions with the longitudinal fractions  $x_1, x_2$  and the transverse impact parameters  $\mathbf{b}_1$  and  $\mathbf{b}_2$ . A further factorisation assumption is to decompose  $\Gamma_{ij}(x_1, x_2, \mathbf{b}_1, \mathbf{b}_2)$  into a longitudinal part and a transverse part

$$\Gamma_{ij}(x_1, x_2, \mathbf{b}_1, \mathbf{b}_2) = D_{ij}(x_1, x_2) T_{ij}(\mathbf{b}_1, \mathbf{b}_2), \quad (2)$$

where  $D_{ij}(x_1, x_2)$  is the double-parton distribution functions (dPDF) [45]. Moreover, by ignoring the correlations between partons produced from each hadrons, one can use

$$\begin{aligned} D_{ij}(x_1, x_2) &= f_i(x_1) f_j(x_2), \\ T_{ij}(\mathbf{b}_1, \mathbf{b}_2) &= T_i(\mathbf{b}_1) T_j(\mathbf{b}_2), \end{aligned} \quad (3)$$

where  $f_i(x_1)$  and  $f_j(x_2)$  are the normal single PDFs. This yields to

$$\sigma_{Q_1 Q_2} = \frac{1}{1 + \delta_{Q_1 Q_2}} \sum_{i,j,k,l} \sigma_{ik \rightarrow Q_1} \sigma_{jl \rightarrow Q_2} \int d^2 \mathbf{b} \int T_i(\mathbf{b}_1) T_k(\mathbf{b}_1 - \mathbf{b}) d^2 \mathbf{b}_1 \int T_j(\mathbf{b}_2) T_l(\mathbf{b}_2 - \mathbf{b}) d^2 \mathbf{b}_2. \quad (4)$$

If one further ignores the parton flavour dependence in  $T_{i,j,k,l}(\mathbf{b})$  and defines the overlapping function

$$F(\mathbf{b}) = \int T(\mathbf{b}_i)T(\mathbf{b}_i - \mathbf{b})d^2\mathbf{b}_i, \quad (5)$$

one reaches the so-called ‘‘pocket formula’’

$$\sigma_{Q_1 Q_2} = \frac{1}{1 + \delta_{Q_1 Q_2}} \frac{\sigma_{Q_1} \sigma_{Q_2}}{\sigma_{\text{eff}}}, \quad (6)$$

where  $\sigma_{Q_1}$  and  $\sigma_{Q_2}$  are the cross sections for respectively single  $Q_1$  and  $Q_2$  production and  $\sigma_{\text{eff}}$  is a parameter to characterise an effective spatial area of the parton-parton interactions via

$$\sigma_{\text{eff}} = \left[ \int d^2\mathbf{b} F(\mathbf{b})^2 \right]^{-1}. \quad (7)$$

Hence, it is only related to the initial states and should be independent of the final state. However, the validation of its universality (process independence as well as energy independence) and the hold of the factorisation in Eq.(6) should be cross checked case by case. Thanks to its larger luminosity and probably wide rapidity coverage, AFTER@LHC provides a unique opportunity to probe DPS and to extract  $\sigma_{\text{eff}}$  from double-quarkonium final states.

To perform our predictions, we will use  $\sigma_{\text{eff}} = 5.0 \pm 2.75$  mb, which was determined from  $J/\psi$ -pair production data at the Tevatron by D0 collaboration [7]. The reason for such a choice is that all of the double-quarkonium production processes share the same gluon-gluon initial states and the typical  $x$  are not that much different. It guarantees that we only need to assume the energy independent of  $\sigma_{\text{eff}}$ . However, we do not claim that this value is the only one possible; we only take it as our reference number. If one wants to use another value of  $\sigma_{\text{eff}}$ , one can just simply perform a rescaling of our presented numbers.

	$\kappa$	$\lambda$	# of data	$\chi^2$		$\kappa$	$\lambda$	# of data	$\chi^2$
$J/\psi$	0.674	0.380	51	422	$\Upsilon(1S)$	0.707	0.0837	288	1883
$\psi(2S)$	0.154	0.351	4	1.12	$\Upsilon(2S)$	0.604	0.0563	205	856
					$\Upsilon(3S)$	0.591	0.0411	197	886

(a) Charmonia (b) Bottomonia

Table 2:  $\chi^2$  results after a combined fit of  $d^2\sigma/dP_T dy$  to (a) the  $\psi(nS)$  PHENIX data [46] by fixing  $n = 2$  and  $\langle P_T \rangle = 4.5$  GeV and (b) the  $\Upsilon(nS)$  data CDF [47], ATLAS [48], CMS [49] and LHCb [50, 51] data by fixing  $n = 2$  and  $\langle P_T \rangle = 13.5$  GeV.

Due to the fact that the description of single heavy quarkonium production at hadron colliders in the whole kinematical region is still a challenge to theorists, using *ab initio* theoretical computation of  $\sigma_Q$  would significantly inflate theoretical uncertainties. Instead, we will work in a data-driven way to determine  $\sigma_Q$ .

Our procedure is as follows. We start from the cross section  $\sigma_{Q_i}$  which can be written as

$$\sigma(pp \rightarrow Q + X) = \sum_{a,b} \int dx_1 dx_2 f_a(x_1) f_b(x_2) \frac{1}{2\hat{s}} |\overline{\mathcal{A}_{ab \rightarrow Q+X}}|^2 d\text{LIPS}_{Q+X}, \quad (8)$$

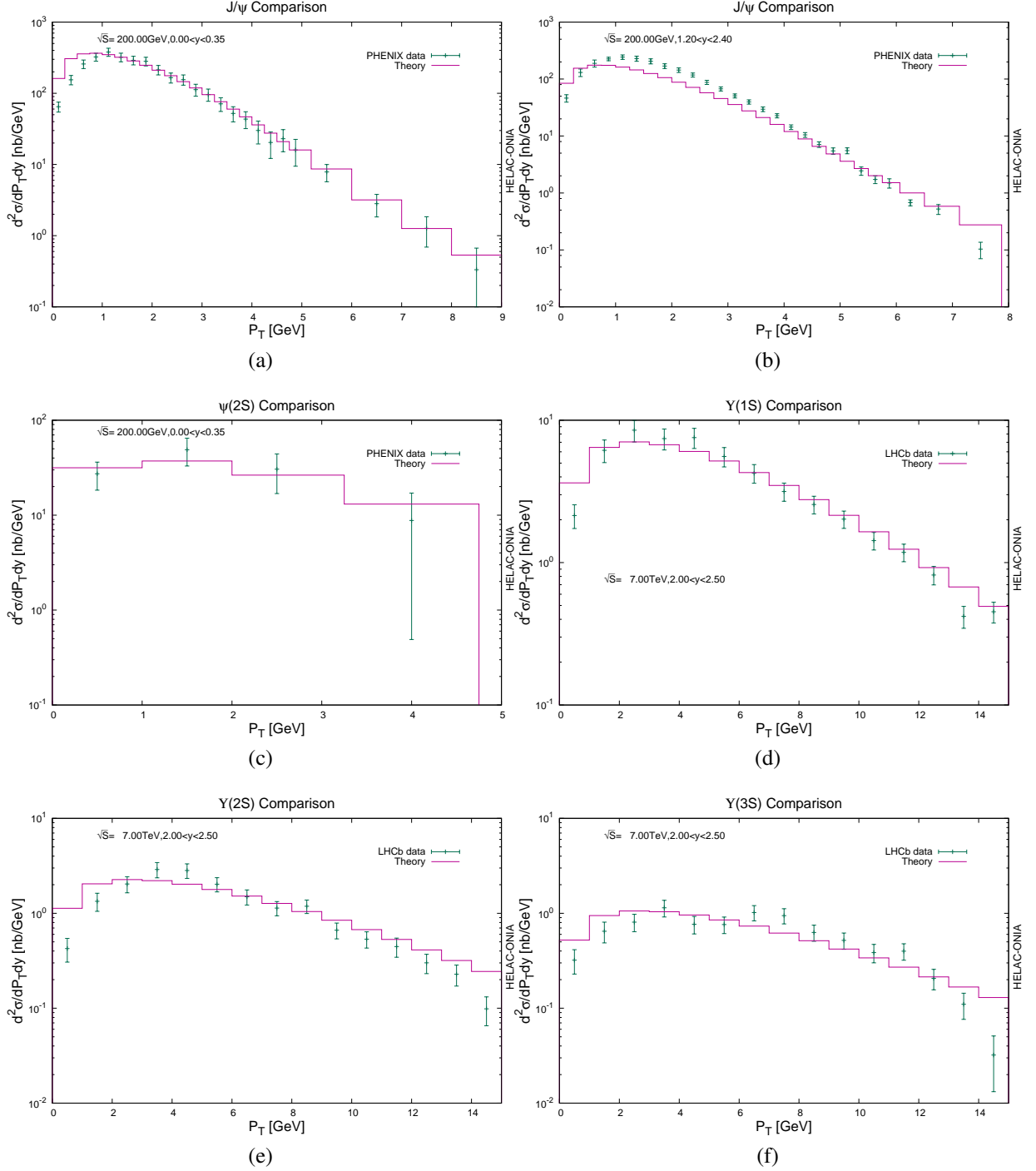


Figure 1: Comparison with PHENIX measurement [46] for  $J/\psi$  (a,b) and  $\psi(2S)$  (c) production and with LHCb measurement [50] for  $\Upsilon(1S)$  (d),  $\Upsilon(2S)$  (e) and  $\Upsilon(3S)$  (f) production

where  $f_a, f_b$  are the parton distribution functions (PDF) of the initial partons  $a$  and  $b$ ,  $dLIPS_{Q+X}$  is the Lorentz-invariant phase space measure for  $pp \rightarrow Q + X$  and  $\hat{s}$  is the partonic centre-of-mass energy (i.e.  $\hat{s} = x_1 x_2 s$ ). For single quarkonium production in  $p + p$  collisions at  $\sqrt{s} = 115$  GeV,

the gluon-gluon initial state is dominant. The initial colour and helicity averaged amplitude square for  $gg \rightarrow Q + X$  can be expressed in the form of a crystal ball function [20]

$$\overline{|\mathcal{A}_{gg \rightarrow Q+X}|^2} = \begin{cases} K \exp(-\kappa \frac{P_T^2}{M_Q^2}) & \text{when } P_T \leq \langle P_T \rangle \\ K \exp(-\kappa \frac{\langle P_T \rangle^2}{M_Q^2}) \left(1 + \frac{\kappa}{n} \frac{P_T^2 - \langle P_T \rangle^2}{M_Q^2}\right)^{-n} & \text{when } P_T > \langle P_T \rangle \end{cases} \quad (9)$$

where  $K = \lambda^2 \kappa \hat{s} / M_Q^2$ . The parameters  $\kappa, \lambda, n$  and  $\langle P_T \rangle$  can be determined by fitting the (differential) cross sections to the experimental data. The dedicated codes to performing the fit and to compute DPS contribution to double-quarkonium production have been implemented in HELAC-ONIA [52].

With the same conditions as in Ref. [20], we reproduced their results. However, after a combined fit of the charmonium data measured at the Tevatron and the LHC, the same parameter set cannot perfectly reproduce the low-energy data measured by PHENIX collaboration [46] at RHIC. Since the collision energy of RHIC  $\sqrt{s} = 200$  GeV is very close to the centre-of-mass energy of the fixed-target experiment at the LHC (AFTER@LHC)  $\sqrt{s} = 115$  GeV, we used the PHENIX data alone to determine the parameters in Eq. (9). A combined fit of  $d^2\sigma/dP_T dy$  to the PHENIX data [46] for  $J/\psi$  and  $\psi(2S)$  production gives the  $\chi^2$  results presented in Tab. 2a having fixed  $n = 2$  and  $\langle P_T \rangle = 4.5$  GeV. We also show the comparisons of the  $P_T$  spectra in Fig. 1a-c.

There is no such measurement of  $\Upsilon$  at RHIC. We therefore performed a combined fit of  $d^2\sigma/dP_T dy$  to CDF [47], ATLAS [48], CMS [49] and LHCb [50, 51] data. The results for  $\Upsilon$  are presented in Tab. 2b having fixed  $n = 2$  and  $\langle P_T \rangle = 13.5$  GeV. For illustration, the comparisons between the fit and the LHCb data [50] are shown in Fig. 1d-f. However, we should recall that the results from the Tevatron/LHC fit may underestimate the RHIC total  $\Upsilon$  production cross section by a factor of 2. Hence, we present the conservative predictions for the corresponding DPS yields of  $\Upsilon$  at AFTER@LHC. All of the above fits are performed with MSTW2008NLO PDF set [53] available in LHAPDF5 [54] and the factorisation scale  $\mu_F = \sqrt{M_Q^2 + P_T^2}$ . The physical mass  $M_Q$  for quarkonium is taken from PDG data [55] as well as the branching ratios.

Once a fit is done,  $|\mathcal{A}_{gg \rightarrow Q+X}|^2$  is fixed allowing us to evaluate  $\sigma(pp \rightarrow Q+X)$  (or its differential counterparts in any variable) which can then be injected into the ‘‘pocket formula’’ Eq. (6) in order to predict the DPS yield. Since we do not apply any muon cuts, we do not need to make any assumptions regarding the polarisation of the production quarkonia.

## 2.2. Single-parton scatterings

### 2.2.1. Double-charmonium and double-bottomonium production

The SPS contribution for  $J/\psi$ -pair production have systematically been investigated in our previous works [16, 18]. We have shown that the leading order (LO) in the strong coupling constant  $\alpha_s$  calculation is enough to account for the low  $P_T$  data as well as the  $P_T$ -integrated cross section, the bulk of the events lying at low  $P_T$ . However, if one goes to mid  $P_T$  (e.g.  $P_T > 5$  GeV),  $\mathcal{O}(\alpha_s^5)$  contribution start to be dominant. As a consequence, the yield and the polarisation changes significantly compared to a LO calculation. Since we are only interested in the data in the low  $P_T$  regime and since our aim is essentially to assess the feasibility of measuring quarkonium pair production with AFTER@LHC, we only perform a LO calculation. Colour-octet contributions in this regime are also negligible: it is suppressed by powers  $v$  without any kinematical enhancement

at variance with the single-quarkonium-production case. Yet, the feed-down contributions from higher excited spin-triplet  $S$ -wave quarkonium might be substantial as already shown for the  $J/\psi$ -pair production in Ref. [18]. We will take these into account. The branching ratios that will be used in this context are taken from PDG [55] and we have listed them in Tab. 3 for completeness.

decay channel	branching ratio (%)	decay channel	branching ratio (%)
$\psi(2S) \rightarrow J/\psi + X$	57.4	$J/\psi \rightarrow \mu^+\mu^-$	5.93
$\Upsilon(2S) \rightarrow \Upsilon(1S) + X$	30.2	$\psi(2S) \rightarrow \mu^+\mu^-$	0.75
$\Upsilon(3S) \rightarrow \Upsilon(1S) + X$	8.92	$\Upsilon(1S) \rightarrow \mu^+\mu^-$	2.48
$\Upsilon(3S) \rightarrow \Upsilon(2S) + X$	10.6	$\Upsilon(2S) \rightarrow \mu^+\mu^-$	1.93
		$\Upsilon(3S) \rightarrow \mu^+\mu^-$	2.18

(a) Decay within a family (b) Leptonic decays

Table 3: Various decays (and branching ratios) considered in this article [55].

The general formula for the amplitude of the production of a pair of colour-singlet (CS)  $S$ -wave quarkonia  $Q_1$  and  $Q_2$  with as initial partons  $a$  and  $b$  is

$$\mathcal{A}_{ab \rightarrow Q_1^{\lambda_1}(P_1) + Q_2^{\lambda_2}(P_2) + X} = \sum_{s_1, s_2, c_1, c_2} \sum_{s_3, s_4, c_3, c_4} \frac{N(\lambda_1|s_1, s_2)N(\lambda_2|s_3, s_4)}{\sqrt{M_{Q_1}M_{Q_2}}} \frac{\delta_{c_1c_2}\delta_{c_3c_4}}{N_c} \frac{R_1(0)R_2(0)}{4\pi} \mathcal{A}_{ab \rightarrow Q_1^{s_1}\bar{Q}_2^{s_2}(\mathbf{p}_1=0) + Q_3^{s_3}\bar{Q}_4^{s_4}(\mathbf{p}_2=0) + X}, \quad (10)$$

where we denote the momenta of quarkonia  $Q_1$  and  $Q_2$  as  $P_1$  and  $P_2$  respectively and their polarisations as  $\lambda_{1,2}$ ,  $N(\lambda_{1,2}|s_{1,3}, s_{2,4})$  are the two spin projectors and  $R_{1,2}(0)$  are the radial wave functions at the origin in the configuration space for both quarkonia. In the above equation, we have defined the heavy-quark momenta to be  $q_{1,2,3,4}$  such that  $P_{1,2} = q_{1,3} + q_{2,4}$  and  $p_{1,2} = (q_{1,3} - q_{2,4})/2$ .  $s_{1,2,3,4}$  are then the heavy-quark spin components and  $\delta_{c_i c_j} / \sqrt{N_c}$  is the colour projector. The spin-triplet projector  $N(\lambda|s_i, s_j)$  has, in the non-relativistic limit,  $v \rightarrow 0$ , the following expression

$$N(\lambda|s_i, s_j) = \frac{\epsilon_\mu^\lambda}{2\sqrt{2}M_Q} \bar{v}\left(\frac{\mathbf{P}}{2}, s_j\right) \gamma^\mu u\left(\frac{\mathbf{P}}{2}, s_i\right). \quad (11)$$

All these computations can be performed automatically in HELAC-ONIA [52] framework based on recursion relations. The radial wave functions at the origin  $R(0)$  are taken from Ref. [56], which were derived in the QCD-motivated Buchmüller-Tye potential [57]. We also listed their values in Tab. 4.

### 2.2.2. Charmonium-bottomonium pair production

The simultaneous production of a charmonium and a bottomonium has been studied in Refs. [13, 19]. Its CSM contributions are expected to be suppressed because the LO contributions in CS mechanism (CSM) are  $\mathcal{O}(\alpha_s^6)$ , i.e.  $\alpha_s^2$  suppressed compared to double-charmonium and double-bottomonium production. Hence, it is expected to be a golden channel to probe colour-octet

mechanism (COM) at the LHC [13]. However, such a statement is valid only if one can clearly separate DPS and SPS events experimentally since the DPS contributions would be dominant. For a thorough discussion, the reader is guided to [19]. In contrast, colour octet (CO) contributions can appear at  $\mathcal{O}(\alpha_s^4)$ , which however are suppressed by the small size of the CO long distance matrix elements (LDMEs). If one follows the arguments of Ref. [13], one is entitled to consider only the  $c\bar{c}({}^3\mathcal{S}_1^{[8]}) + b\bar{b}({}^3\mathcal{S}_1^{[8]})$ ,  $c\bar{c}({}^3\mathcal{S}_1^{[1]}) + b\bar{b}({}^3\mathcal{S}_1^{[8]})$  and  $c\bar{c}({}^3\mathcal{S}_1^{[8]}) + b\bar{b}({}^3\mathcal{S}_1^{[1]})$  channels. This approximation is however based on the validity of the velocity scaling rules of the LDMEs which may not be that reliable. Since we have also followed this approximation, our SPS results for charmonium-bottomonium production should only be considered as a rough estimate of the yields.

The formula of the amplitude is similar to that of CS state production with the following replacements for CO in Eq.(11)

$$\frac{\delta_{c_i, c_j}}{\sqrt{N_c}} \rightarrow \sqrt{2} T_{c_i c_j}^a, \quad \frac{R_i(0)}{\sqrt{4\pi}} \rightarrow \frac{\sqrt{\langle \mathcal{O}^i({}^3\mathcal{S}_1^{[8]}) \rangle}}{\sqrt{3(N_c^2 - 1)}}, \quad (12)$$

where  $T_{c_i c_j}^a$  is the Gell-Mann matrix and  $\langle \mathcal{O}^i({}^3\mathcal{S}_1^{[8]}) \rangle$  is the CO LDME.

The CO LDMEs  $\langle \mathcal{O}^i({}^3\mathcal{S}_1^{[8]}) \rangle$  should be determined from experimental data. We took the values from a LO fit to the large  $P_T$  data as described in Refs. [58, 59, 60] as our reference numbers; these are consistent with those used in Refs.[13, 19]. The values of  $\langle \mathcal{O}({}^3\mathcal{S}_1^{[8]}) \rangle$  for various heavy quarkonia are presented in Tab. 4. We will not include the feed-down contributions and  $\mathcal{O}(\alpha_s^6)$  CS contributions here. As already shown in Ref. [19], the feed-down contributions from  $\chi_c \chi_b$  and the partial  $\mathcal{O}(\alpha_s^6)$  CS contributions are indeed small.

Quarkonium	$ R(0) ^2$ (GeV <sup>3</sup> )	$\langle \mathcal{O}({}^3\mathcal{S}_1^{[8]}) \rangle$ (GeV <sup>3</sup> )
$J/\psi$	0.81	$3.9 \times 10^{-3}$
$\psi(2S)$	0.529	$3.7 \times 10^{-3}$
$\Upsilon(1S)$	6.477	$1.5 \times 10^{-1}$
$\Upsilon(2S)$	3.234	$4.5 \times 10^{-2}$
$\Upsilon(3S)$	2.474	$7.5 \times 10^{-2}$

Table 4: The radial wave functions at the origin squared  $|R(0)|^2$  [56] and the CO LDMEs  $\langle \mathcal{O}({}^3\mathcal{S}_1^{[8]}) \rangle$  [58, 59, 60] involved in this article.

Finally, we describe our parameters for our SPS calculations. In the non-relativistic limit, the mass of heavy quarkonium can be expressed as the sum of the corresponding heavy-quark-pair masses. In our case, we have

$$M_Q = 2m_Q, \quad (13)$$

where  $m_Q = m_c$  for charmonium and  $m_Q = m_b$  for bottomonium. The masses of charm quark and bottom quark are taken as  $m_c = 1.5 \pm 0.1$  GeV and  $m_b = 4.75 \pm 0.25$  GeV. The factorisation scale  $\mu_F$  and the renormalisation scale  $\mu_R$  are taken as  $\mu_F = \mu_R \in [\frac{1}{2}\mu_0, 2\mu_0]$  with  $\mu_0 = \sqrt{(M_{Q_1} + M_{Q_2})^2 + P_T^2}$ . The advantage of using  $\mu_0 = \sqrt{(M_{Q_1} + M_{Q_2})^2 + P_T^2}$  is that we are

able to recover the correct mass threshold  $M_{Q_1} + M_{Q_2}$  in the low  $P_T$  regime. Finally, the PDF set for the SPS calculation is CTEQ6L1 [61] with the one-loop renormalisation group running of  $\alpha_s$ .

### 3. Energy dependence of the ratio DPS over SPS

Due to the very large integrated luminosity of AFTER@LHC (up to  $20 \text{ fb}^{-1}$  per year) compared to the experiments performed at RHIC, the measurement of double-quarkonium production at AFTER@LHC will provide a unique test of the interplay between the DPS and SPS production mechanisms in a new energy range. The energy dependence of  $\sigma_{\text{eff}}$  will be explored at a wide energy range when combined with the LHC collider and Tevatron data. Due to the double enhancement of the initial gluon-gluon luminosity with the energy,  $\sqrt{s}$ , DPS contributions are expected to be more and more important with respect to the SPS ones at larger  $\sqrt{s}$ . This can be observed on Fig. 2. The fact that we have used a crystal ball fit on the partonic amplitude ( $gg \rightarrow QX$ ) to the Tevatron and LHC data to perform the DPS predictions allows us to predict the non-trivial energy (and rapidity) dependence of the DPS predictions.

One however sees on Fig. 2 that a change of  $\sigma_{\text{eff}}$  from 15 mb –which seems to be the favoured value for jet-related observables– to 5mb –which is the value extracted by D0 from the  $J/\psi + J/\psi$  data [7]– results in a significant change in the point where both contributions are equal. In the former case, it occurs very close to the energy of AFTER@LHC, in the latter case, it occurs between the Tevatron and the LHC energies. All this clearly motivates for measurement and  $\sigma_{\text{eff}}$  extractions at low energies.

### 4. Predictions at AFTER@LHC

We are now in the position to present our numerical results at  $\sqrt{s} = 115 \text{ GeV}$  in  $p+p$  collisions. The total cross section we obtained are given in Tab. 5, 6 and 7. The results have been multiplied by the branching ratios into a muon pair and they are all in unit of fb. In general, we have

$$\sigma^{\Upsilon\Upsilon \rightarrow 4\mu} \ll \sigma^{\psi\Upsilon \rightarrow 4\mu} \ll \sigma^{\psi\psi \rightarrow 4\mu}. \quad (14)$$

The DPS contributions decrease quickly when the mass threshold  $M_{Q_1} + M_{Q_2}$  increases because of its square dependence of the initial-state parton luminosity. With the nominal integrated luminosity of  $20 \text{ fb}^{-1}$  proposed to be collected at AFTER@LHC, we find that the measurement double-bottomonium production is out of reach<sup>2</sup> and one may be able to record a few  $J/\psi + \Upsilon(1S)$  events, which are DPS dominated. However, one should always keep in mind that  $\sigma_{\text{SPS}}$  for  $\psi + \Upsilon$  production strongly depends on the CO LDMEs  $\langle O(\mathcal{S}_1^{[8]}) \rangle$ . An upper limit determination would already be insightful. The quoted theoretical uncertainties include  $\sigma_{\text{eff}} = 5 \pm 2.75 \text{ mb}$  for the DPS yields and scale uncertainties as well as heavy quark mass uncertainties for the SPS yields, which were already discussed in Sec.2.

As regards double-charmonium production, about 10 thousand events could be collected per year –which is more than what has so far been collected by LHCb and CMS. In the analysis

---

<sup>2</sup>We note that such a measurement has never been done anywhere else.

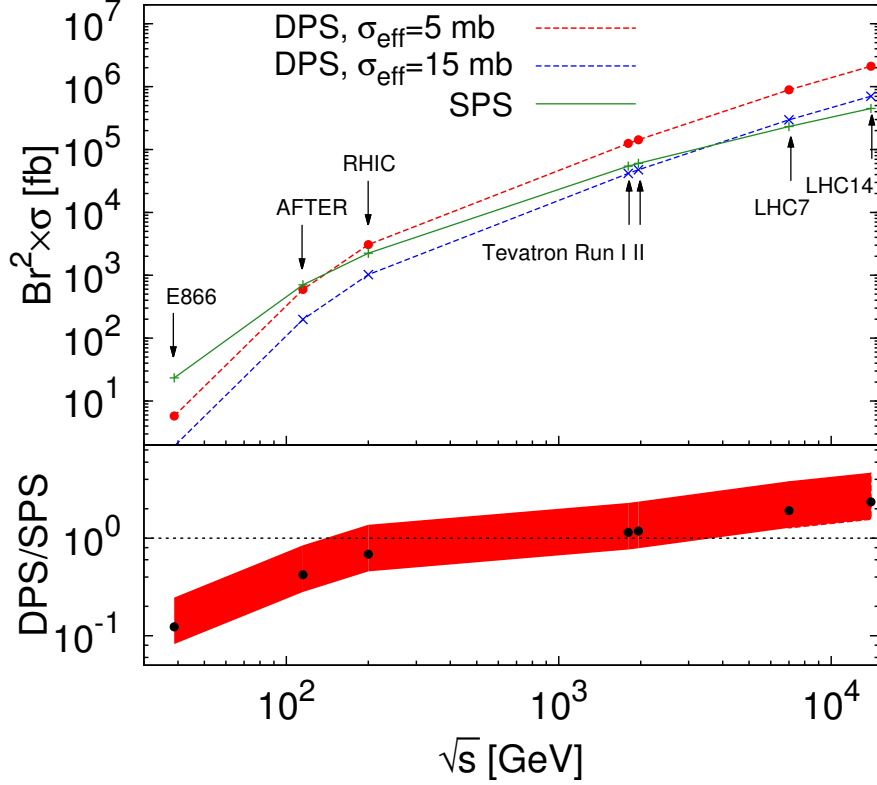


Figure 2: (Upper panel) The cross sections of (prompt-) $J/\psi$  pair production via SPS and DPS mechanisms for two values of  $\sigma_{\text{eff}}$  as a function of  $\sqrt{s}$ . (Lower panel) DPS over SPS yield ratio for  $5 < \sigma_{\text{eff}} < 15$  mb. The black circles correspond to 10 mb. [Aside from the choice of  $\sigma_{\text{eff}}$ , no theoretical uncertainties are included].

of the differential distributions, we therefore only focus on these and, in particular, on  $J/\psi$ -pair production. In Fig. 3, we show three interesting distributions without kinematical cuts. Along the lines of [39], we also used the LHCb kinematical acceptance, *i.e.* the rapidity of  $J/\psi$  restricted to be in the interval of [2, 5]. The corresponding distributions are shown in Fig. 4.

	$\Upsilon(1S) + \Upsilon(1S)$	$\Upsilon(2S) + \Upsilon(2S)$	$\Upsilon(3S) + \Upsilon(3S)$
$\sigma_{\text{DPS}}$	$1.14 \cdot 10^{-5} \begin{smallmatrix} +1.39 \cdot 10^{-5} \\ -4.03 \cdot 10^{-6} \end{smallmatrix}$	$5.54 \cdot 10^{-7} \begin{smallmatrix} +6.77 \cdot 10^{-7} \\ -1.96 \cdot 10^{-7} \end{smallmatrix}$	$1.32 \cdot 10^{-7} \begin{smallmatrix} +1.62 \cdot 10^{-7} \\ -4.70 \cdot 10^{-8} \end{smallmatrix}$
$\sigma_{\text{SPS}}$	$2.78 \cdot 10^{-3} \begin{smallmatrix} +1.31 \cdot 10^{-2} \\ -2.20 \cdot 10^{-3} \end{smallmatrix}$	$3.49 \cdot 10^{-4} \begin{smallmatrix} +1.65 \cdot 10^{-3} \\ -2.77 \cdot 10^{-4} \end{smallmatrix}$	$2.23 \cdot 10^{-4} \begin{smallmatrix} +1.05 \cdot 10^{-3} \\ -1.77 \cdot 10^{-4} \end{smallmatrix}$
	$\Upsilon(1S) + \Upsilon(2S)$	$\Upsilon(1S) + \Upsilon(3S)$	$\Upsilon(2S) + \Upsilon(3S)$
$\sigma_{\text{DPS}}$	$5.02 \cdot 10^{-6} \begin{smallmatrix} +6.13 \cdot 10^{-6} \\ -1.78 \cdot 10^{-6} \end{smallmatrix}$	$2.45 \cdot 10^{-6} \begin{smallmatrix} +3.00 \cdot 10^{-6} \\ -8.71 \cdot 10^{-7} \end{smallmatrix}$	$5.41 \cdot 10^{-7} \begin{smallmatrix} +6.62 \cdot 10^{-7} \\ -1.92 \cdot 10^{-7} \end{smallmatrix}$
$\sigma_{\text{SPS}}$	$1.97 \cdot 10^{-3} \begin{smallmatrix} +9.29 \cdot 10^{-3} \\ -1.56 \cdot 10^{-3} \end{smallmatrix}$	$1.57 \cdot 10^{-3} \begin{smallmatrix} +7.43 \cdot 10^{-3} \\ -1.25 \cdot 10^{-3} \end{smallmatrix}$	$5.58 \cdot 10^{-4} \begin{smallmatrix} +2.63 \cdot 10^{-3} \\ -4.43 \cdot 10^{-4} \end{smallmatrix}$

Table 5:  $\sigma(pp \rightarrow Q_1 + Q_2 + X) \times \mathcal{B}(Q_1 \rightarrow \mu^+\mu^-)\mathcal{B}(Q_2 \rightarrow \mu^+\mu^-)$  in units of fb with  $\sqrt{s} = 115$  GeV, where  $Q_1, Q_2 = \Upsilon(1S), \Upsilon(2S), \Upsilon(3S)$ .

	$J/\psi + \Upsilon(1S)$	$J/\psi + \Upsilon(2S)$	$J/\psi + \Upsilon(3S)$
$\sigma_{\text{DPS}}$	$0.164^{+0.201}_{-0.0583}$	$0.0362^{+0.0443}_{-0.0129}$	$0.0177^{+0.0217}_{-0.00629}$
$\sigma_{\text{SPS}}$	$6.11 \cdot 10^{-3} \begin{smallmatrix} +3.01 \cdot 10^{-2} \\ -4.88 \cdot 10^{-3} \end{smallmatrix}$	$1.75 \cdot 10^{-3} \begin{smallmatrix} +8.64 \cdot 10^{-3} \\ -1.40 \cdot 10^{-3} \end{smallmatrix}$	$2.47 \cdot 10^{-3} \begin{smallmatrix} +1.21 \cdot 10^{-2} \\ -1.97 \cdot 10^{-3} \end{smallmatrix}$
	$\psi(2S) + \Upsilon(1S)$	$\psi(2S) + \Upsilon(2S)$	$\psi(2S) + \Upsilon(3S)$
$\sigma_{\text{DPS}}$	$2.57 \cdot 10^{-3} \begin{smallmatrix} +3.14 \cdot 10^{-3} \\ -9.12 \cdot 10^{-4} \end{smallmatrix}$	$5.67 \cdot 10^{-4} \begin{smallmatrix} +6.93 \cdot 10^{-4} \\ -2.01 \cdot 10^{-4} \end{smallmatrix}$	$2.77 \cdot 10^{-4} \begin{smallmatrix} +3.39 \cdot 10^{-4} \\ -9.84 \cdot 10^{-5} \end{smallmatrix}$
$\sigma_{\text{SPS}}$	$6.09 \cdot 10^{-4} \begin{smallmatrix} +3.00 \cdot 10^{-3} \\ -4.86 \cdot 10^{-4} \end{smallmatrix}$	$1.82 \cdot 10^{-4} \begin{smallmatrix} +8.96 \cdot 10^{-4} \\ -1.45 \cdot 10^{-4} \end{smallmatrix}$	$2.41 \cdot 10^{-4} \begin{smallmatrix} +1.19 \cdot 10^{-3} \\ -1.93 \cdot 10^{-4} \end{smallmatrix}$

Table 6:  $\sigma(pp \rightarrow Q_1 + Q_2 + X) \times \mathcal{B}(Q_1 \rightarrow \mu^+ \mu^-) \mathcal{B}(Q_2 \rightarrow \mu^+ \mu^-)$  in units of fb with  $\sqrt{s} = 115$  GeV, where  $Q_1 = J/\psi, \psi(2S)$  and  $Q_2 = \Upsilon(1S), \Upsilon(2S), \Upsilon(3S)$ .

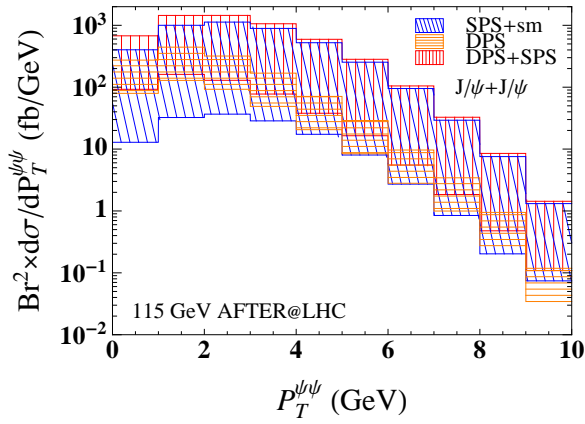
	$J/\psi + J/\psi$	$J/\psi + \psi(2S)$	$\psi(2S) + \psi(2S)$
$\sigma_{\text{DPS}}$	$594^{+725}_{-211}$	$18.6^{+22.7}_{-6.59}$	$0.145^{+0.177}_{-0.0515}$
$\sigma_{\text{SPS}}$	$703^{+3627}_{-564}$	$84.5^{+436}_{-67.7}$	$2.54^{+13.1}_{-2.03}$

Table 7:  $\sigma(pp \rightarrow Q_1 + Q_2 + X) \times \mathcal{B}(Q_1 \rightarrow \mu^+ \mu^-) \mathcal{B}(Q_2 \rightarrow \mu^+ \mu^-)$  in units of fb at  $\sqrt{s} = 115$  GeV, where  $Q_1, Q_2 = J/\psi, \psi(2S)$ .

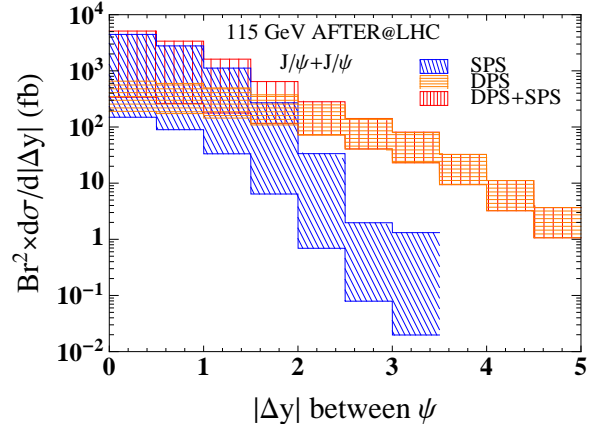
As we already discussed in Ref.[18], at LO, a  $2 \rightarrow 2$  kinematics for SPS would result in the transverse momentum of the  $J/\psi$ -pair  $P_T^{\psi\psi}$  to be zero. However, it can be smeared by the intrinsic  $k_T$  of the initial partons. We accounted for such an effect with a Gaussian distribution with  $\langle k_T \rangle = 2$  GeV as also done in Refs. [16, 18]. However, due to the relative smaller yields at AFTER@LHC than at CMS, one can only access to  $P_T^{\psi\psi} < 10$  GeV regime, which can be clearly seen from Fig. 3a and Fig. 4a. In such a kinematical region, the  $k_T$  smearing effect makes the spectrum of SPS as broad as the DPS one. This difference mostly depends on the value of  $\langle k_T \rangle$  which is essentially empirical.

The absolute rapidity difference between the  $J/\psi$  pair is expected to be a good observable to discriminate the DPS and SPS contributions. This was first pointed out in Ref. [20] and this was used later on by D0 collaboration [7] to extract  $\sigma_{\text{eff}}$  from double- $J/\psi$  production at the Tevatron. The DPS events should have a broader distribution in  $\Delta y$  than the SPS ones, because two (relatively) independent hard interactions happen simultaneously in DPS while the two  $J/\psi$  from SPS are more correlated. The situation still does not change at AFTER@LHC with or without cut as Fig. 3b and Fig. 4b show. In the latter case, the restriction to negative rapidities in the centre-of-mass obviously reduce the  $\Delta y$  range (see Fig. 4b). Starting from  $\Delta y = 2$ , the DPS events dominate the SPS events. A ratio DPS/SPS of 10 is obtained for  $\Delta y > 2$ . The distribution of the invariant mass for the  $J/\psi$  pair  $M_{\psi\psi}$  reflects a similar information as the  $\Delta y$  distribution. Hence, it follows that the  $M_{\psi\psi}$  spectra of DPS are also broader than those of SPS, which can be seen on Fig. 3c and Fig. 4c.

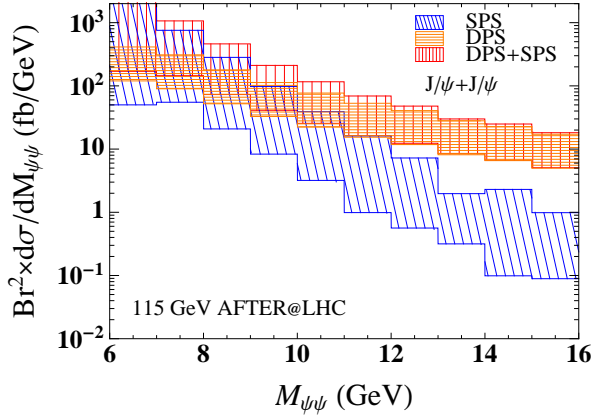
Finally, we present the cross section as a function of the total rapidity of the  $J/\psi$  pair,  $Y_{\psi\psi}$ , and of the sub-leading  $P_T$  between the  $J/\psi$  pair in Fig. 3d and Fig. 4d. One sees that the sub-leading  $P_T$



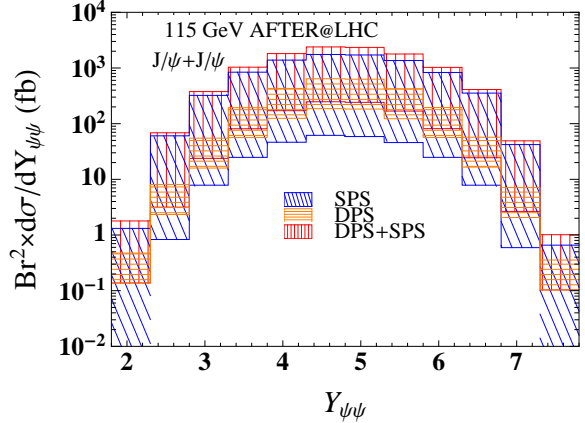
(a) Transverse momentum spectrum



(b) Absolute rapidity difference between  $J/\psi$  pair



(c) Invariant mass distribution



(d) Rapidity of  $J/\psi$  pair

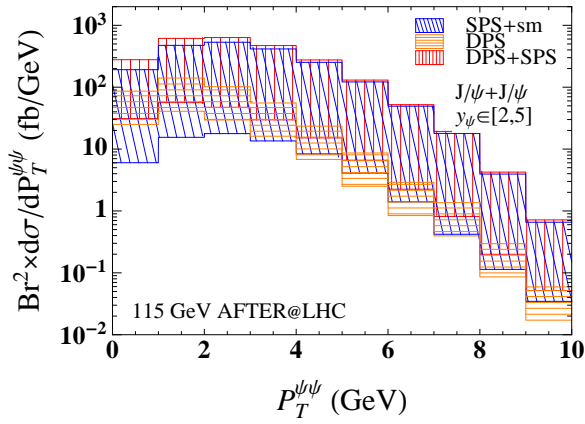
Figure 3: Differential distributions:(a) transverse momentum spectrum; (b) absolute rapidity difference ; (c) invariant mass distribution; (d) rapidity of  $J/\psi$  pair.

spectrum may be measured up to 6 GeV with AFTER@LHC. As regards the rapidity distribution, its maximum is obviously located at  $Y_{\text{cms}} = 0$ , that is  $Y = 4.8$  in the lab frame. One sees that one can expect some counts down to  $Y_{\psi\psi} \simeq 2.5$  where  $x_F \simeq \frac{2M_{\psi\psi}}{\sqrt{s}} \sinh(Y_{\psi\psi} - 4.8) \simeq -0.5$ . This is precisely the kinematical region where double intrinsic  $c\bar{c}$  coalescence contributes on average [10]. Any modulation in the pair-rapidity distribution would sign the presence of such a contribution.

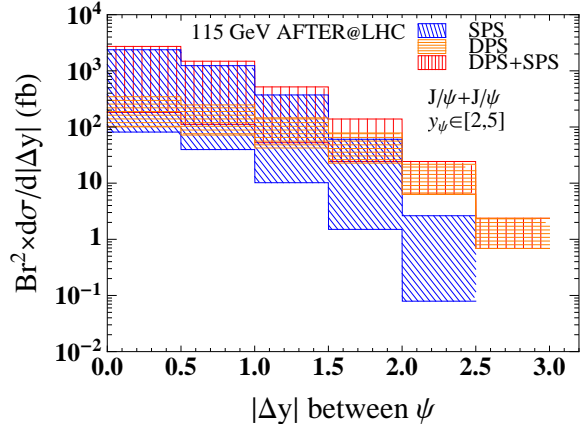
The systematical dependencies of various (d)PDFs (MSTW2008NLO [53], CTEQ6L1 [61], GS09 dPDF [45]) on differential distributions are also shown in Fig. 5; they are found to be moderate in all cases.

## 5. Conclusion

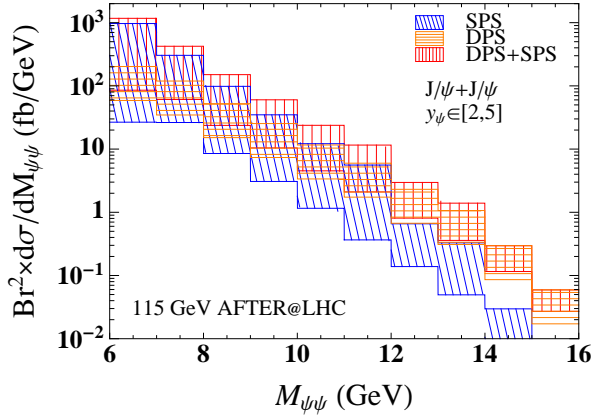
We have discussed double-quarkonium production in proton-proton collisions at a fixed-target experiment using the LHC proton beams, AFTER@LHC. These processes have lately attracted much attention, both in the theorist and experimentalist communities. They are expected to be



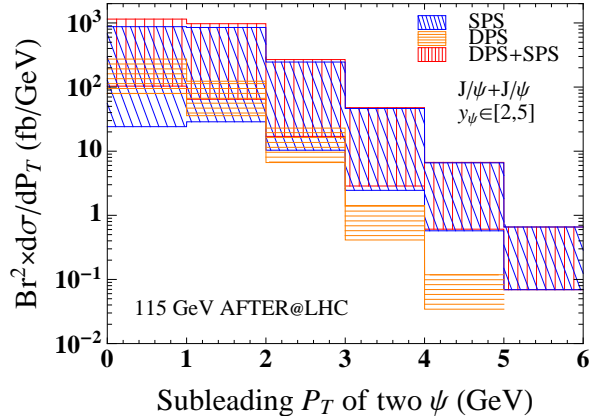
(a) Transverse momentum spectrum



(b) Absolute rapidity difference between  $J/\psi$  pair



(c) Invariant mass distribution

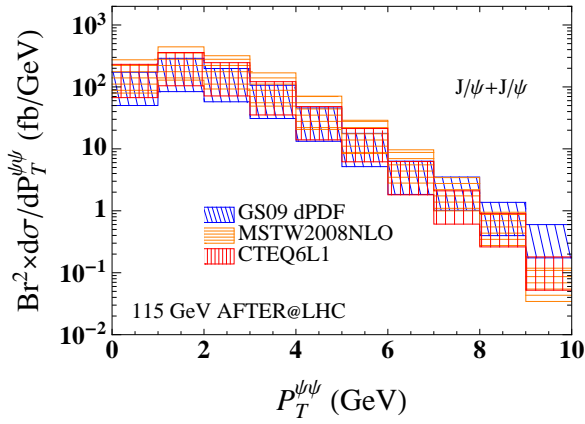


(d) Sub-leading  $P_T$  between  $J/\psi$  pair

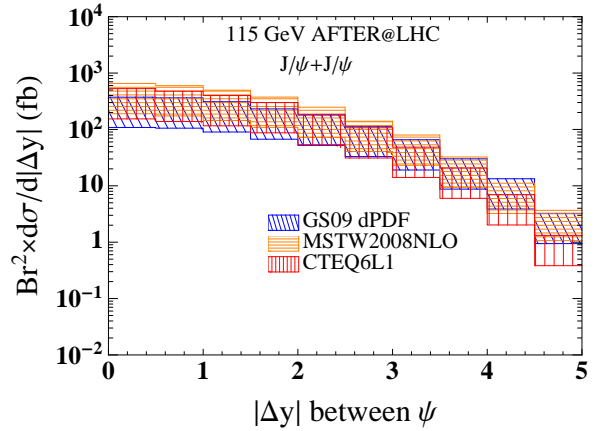
Figure 4: Differential distributions with cut  $2 < y_{J/\psi} < 5$ : (a) transverse momentum spectrum; (b) absolute rapidity difference; (c) invariant mass distribution; (d) sub-leading  $P_T$ .

good observables to further constrain the various models describing heavy-quarkonium production. Double-quarkonium production also provides a good opportunity to study DPS since the yields of single quarkonium production is large and their decay to four muons is a clean signal at a hadron colliders. AFTER@LHC provides very appealing opportunities to study these observables with a LHCb-like detector and in new energy region.

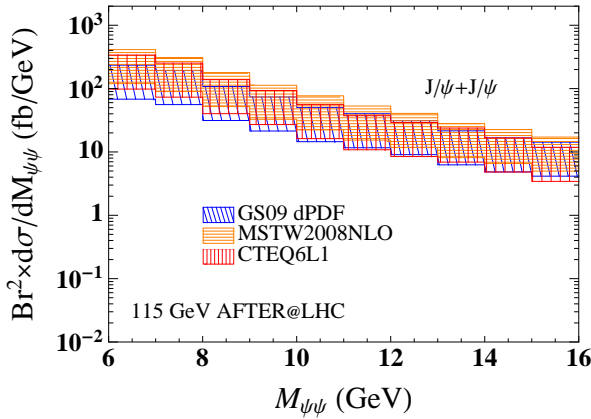
In this paper, we have studied both DPS and SPS contributions for double-quarkonium production. These processes include  $\psi(n_1 S) + \psi(n_2 S)$ ,  $\psi(n_1 S) + \Upsilon(m_1 S)$  and  $\Upsilon(m_1 S) + \Upsilon(m_2 S)$  with  $n_1, n_2 = 1, 2$  and  $m_1, m_2 = 1, 2, 3$ . DPS contributions are estimated in a data-driven way, while SPS ones are calculated in LO non-relativistic QCD [62]. From our calculations, we find that ten thousand of double-charmonium events can indeed be measured at AFTER@LHC with the yearly integrated luminosity of  $20 \text{ fb}^{-1}$ . In the most backward region, a careful analysis of the rapidity distribution could also uncover double intrinsic  $c\bar{c}$  coalescence contributions. In general, future measurements on double-charmonium production can provide extremely valuable information on QCD, in particular important tests on the factorisation formula for DPS and the energy



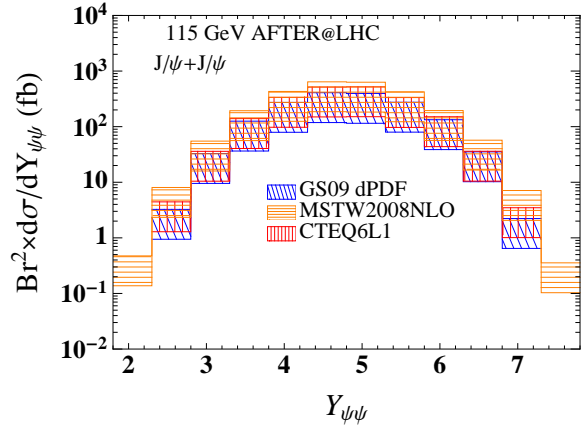
(a) Transverse momentum spectrum



(b) Absolute rapidity difference between  $J/\psi$  pair



(c) Invariant mass distribution



(d) Rapidity of  $J/\psi$  pair

Figure 5: Differential distributions for DPS with various PDFs:(a) transverse momentum spectrum; (b) absolute rapidity difference ; (c) invariant mass distribution; (d) rapidity of  $J/\psi$  pair.

(in)dependence of  $\sigma_{\text{eff}}$ .

## Acknowledgements

This work is supported in part by the France-China Particle Physics Laboratory (FCPPL) and by the French CNRS via the grants PICS-06149 Torino-IPNO, FCPPL-Quarkonium4AFTER & PEPS4AFTER2. H.-S. Shao is also supported by the ERC grant 291377 “LHCtheory: Theoretical predictions and analyses of LHC physics: advancing the precision frontier”.

## References

- [1] N. Brambilla, S. Eidelman, B. Heltsley, R. Vogt, G. Bodwin, *et al.*, “Heavy quarkonium: progress, puzzles, and opportunities,” *Eur.Phys.J.* **C71** (2011) 1534, [arXiv:1010.5827](https://arxiv.org/abs/1010.5827) [hep-ph].
- [2] J. P. Lansberg, “ $J/\psi$ ,  $\psi'$  and  $\Upsilon$  production at hadron colliders: A Review,” *Int.J.Mod.Phys.* **A21** (2006) 3857–3916, [arXiv:hep-ph/0602091](https://arxiv.org/abs/hep-ph/0602091) [hep-ph].

- [3] S. Brodsky, F. Fleuret, C. Hadjidakis, and J. P. Lansberg, “Physics Opportunities of a Fixed-Target Experiment using the LHC Beams,” *Phys.Rept.* **522** (2013) 239–255, [arXiv:1202.6585 \[hep-ph\]](#).
- [4] ATLAS Collaboration, G. Aad *et al.*, “Measurement of the production cross section of prompt  $J/\psi$  mesons in association with a  $W^\pm$  boson in  $pp$  collisions at  $\sqrt{s} = 7$  TeV with the ATLAS detector,” *JHEP* **1404** (2014) 172, [arXiv:1401.2831 \[hep-ex\]](#).
- [5] ATLAS Collaboration, G. Aad *et al.*, “Observation and measurements of the production of prompt and non-prompt  $J/\psi$  mesons in association with a Z boson in  $pp$  collisions at  $\sqrt{s} = 8$  TeV with the ATLAS detector,” [arXiv:1412.6428 \[hep-ex\]](#).
- [6] LHCb Collaboration, R. Aaij *et al.*, “Observation of double charm production involving open charm in  $pp$  collisions at  $\sqrt{s} = 7$  TeV,” *JHEP* **1206** (2012) 141, [arXiv:1205.0975 \[hep-ex\]](#).
- [7] D0 Collaboration, V. M. Abazov *et al.*, “Observation and studies of double  $J/\psi$  production at the Tevatron,” *Phys.Rev.* **D90** no. 11, (2014) 111101, [arXiv:1406.2380 \[hep-ex\]](#).
- [8] V. Kartvelishvili and S. Esakiya, “ON HADRON INDUCED PRODUCTION OF J / PSI MESON PAIRS. (IN RUSSIAN),” *Yad.Fiz.* **38** (1983) 722–726.
- [9] B. Humpert and P. Mery, “psi psi PRODUCTION AT COLLIDER ENERGIES,” *Z.Phys.* **C20** (1983) 83.
- [10] R. Vogt and S. Brodsky, “Intrinsic charm contribution to double quarkonium hadroproduction,” *Phys.Lett.* **B349** (1995) 569–575, [arXiv:hep-ph/9503206 \[hep-ph\]](#).
- [11] R. Li, Y.-J. Zhang, and K.-T. Chao, “Pair Production of Heavy Quarkonium and B(c)(\*) Mesons at Hadron Colliders,” *Phys.Rev.* **D80** (2009) 014020, [arXiv:0903.2250 \[hep-ph\]](#).
- [12] C.-F. Qiao, L.-P. Sun, and P. Sun, “Testing Charmonium Production Mechanism via Polarized J/psi Pair Production at the LHC,” *J.Phys.* **G37** (2010) 075019, [arXiv:0903.0954 \[hep-ph\]](#).
- [13] P. Ko, C. Yu, and J. Lee, “Inclusive double-quarkonium production at the Large Hadron Collider,” *JHEP* **1101** (2011) 070, [arXiv:1007.3095 \[hep-ph\]](#).
- [14] A. Berezhnoy, A. Likhoded, A. Luchinsky, and A. Novoselov, “Double J/psi-meson Production at LHC and 4c-tetraquark state,” *Phys.Rev.* **D84** (2011) 094023, [arXiv:1101.5881 \[hep-ph\]](#).
- [15] Y.-J. Li, G.-Z. Xu, K.-Y. Liu, and Y.-J. Zhang, “Relativistic Correction to  $J/\psi$  and  $\Upsilon$  Pair Production,” *JHEP* **1307** (2013) 051, [arXiv:1303.1383 \[hep-ph\]](#).
- [16] J.-P. Lansberg and H.-S. Shao, “Production of  $J/\psi + \eta_c$  versus  $J/\psi + J/\psi$  at the LHC: Importance of Real  $\alpha_s^5$  Corrections,” *Phys.Rev.Lett.* **111** (2013) 122001, [arXiv:1308.0474 \[hep-ph\]](#).
- [17] L.-P. Sun, H. Han, and K.-T. Chao, “Impact of  $J/\psi$  pair production at the LHC and predictions in nonrelativistic QCD,” [arXiv:1404.4042 \[hep-ph\]](#).
- [18] J.-P. Lansberg and H.-S. Shao, “ $J/\psi$ -Pair Production at Large Momenta: Indications for Double-Parton Scatterings and Large  $\alpha_s^5$  Contributions,” [arXiv:1410.8822 \[hep-ph\]](#).
- [19] A. Likhoded, A. Luchinsky, and S. Poslavsky, “Simultaneous production of charmonium and bottomonium mesons at LHC,” [arXiv:1503.00246 \[hep-ph\]](#).
- [20] C. Kom, A. Kulesza, and W. Stirling, “Pair Production of J/psi as a Probe of Double Parton Scattering at LHCb,” *Phys.Rev.Lett.* **107** (2011) 082002, [arXiv:1105.4186 \[hep-ph\]](#).
- [21] S. Baranov, A. Snigirev, and N. Zotov, “Double heavy meson production through double parton scattering in hadronic collisions,” *Phys.Lett.* **B705** (2011) 116–119, [arXiv:1105.6276 \[hep-ph\]](#).
- [22] A. Berezhnoy, A. Likhoded, A. Luchinsky, and A. Novoselov, “Double  $c\bar{c}$  production at LHCb,” *Phys.Rev.* **D86** (2012) 034017, [arXiv:1204.1058 \[hep-ph\]](#).
- [23] S. Baranov, A. Snigirev, N. Zotov, A. Szczurek, and W. Schfer, “Interparticle correlations in the production of  $J/\psi$  pairs in proton-proton collisions,” *Phys.Rev.* **D87** no. 3, (2013) 034035, [arXiv:1210.1806 \[hep-ph\]](#).
- [24] D. d’Enterria and A. M. Snigirev, “Enhanced J/Psi production from double parton scatterings in nucleus-nucleus collisions at the Large Hadron Collider,” *Phys.Lett.* **B727** (2013) 157–162, [arXiv:1301.5845 \[hep-ph\]](#).
- [25] D. d’Enterria and A. M. Snigirev, “Pair production of quarkonia and electroweak bosons from double-parton scatterings in nuclear collisions at the LHC,” *Nucl.Phys.* **A931** (2014) 303–308, [arXiv:1408.5172 \[hep-ph\]](#).
- [26] LHCb Collaboration, R. Aaij *et al.*, “Observation of  $J/\psi$  pair production in  $pp$  collisions at  $\sqrt{s} = 7$  TeV,”

- Phys.Lett.* **B707** (2012) 52–59, [arXiv:1109.0963 \[hep-ex\]](#).
- [27] CMS Collaboration, V. Khachatryan *et al.*, “Measurement of prompt  $J/\psi$  pair production in pp collisions at  $\sqrt{s} = 7$  TeV,” *JHEP* **1409** (2014) 094, [arXiv:1406.0484 \[hep-ex\]](#).
- [28] J. P. Lansberg, S. Brodsky, F. Fleuret, and C. Hadjidakis, “Quarkonium Physics at a Fixed-Target Experiment using the LHC Beams,” *Few Body Syst.* **53** (2012) 11–25, [arXiv:1204.5793 \[hep-ph\]](#).
- [29] T. Liu and B.-Q. Ma, “Azimuthal asymmetries in lepton-pair production at a fixed-target experiment using the LHC beams (AFTER),” *Eur.Phys.J.* **C72** (2012) 2037, [arXiv:1203.5579 \[hep-ph\]](#).
- [30] D. Boer and C. Pisano, “Polarized gluon studies with charmonium and bottomonium at LHCb and AFTER,” *Phys.Rev.* **D86** (2012) 094007, [arXiv:1208.3642 \[hep-ph\]](#).
- [31] G. Chen, X.-G. Wu, J.-W. Zhang, H.-Y. Han, and H.-B. Fu, “Hadronic production of  $\Xi_{cc}$  at a fixed-target experiment at the LHC,” *Phys.Rev.* **D89** no. 7, (2014) 074020, [arXiv:1401.6269 \[hep-ph\]](#).
- [32] K. Kanazawa, Y. Koike, A. Metz, and D. Pitonyak, “Transverse single-spin asymmetries in proton-proton collisions at the AFTER@LHC experiment,” [arXiv:1502.04021 \[hep-ph\]](#).
- [33] R. E. Mikkelsen, A. H. Srensen, and U. I. Uggerhj, “Bremsstrahlung from relativistic heavy ions in a fixed target experiment at the LHC,” [arXiv:1503.06621 \[nucl-ex\]](#).
- [34] V. Goncalves and W. Sauter, “ $\eta_c$  production in photon - induced interactions at the AFTER@LHC experiment as a probe of the Odderon,” [arXiv:1503.05112 \[hep-ph\]](#).
- [35] J. P. Lansberg, L. Szymanowski, and J. Wagner, “Lepton-pair production in ultraperipheral collisions at AFTER@LHC,” [arXiv:1504.02733 \[hep-ph\]](#).
- [36] F. A. Ceccopieri, “Studies of backward particle production with A Fixed-Target Experiment using the LHC beams,” [arXiv:1503.05813 \[hep-ph\]](#).
- [37] M. Anselmino, U. D’Alesio, and S. Melis, “Transverse single-spin asymmetries in proton-proton collisions at the AFTER@LHC experiment in a TMD factorisation scheme,” [arXiv:1504.03791 \[hep-ph\]](#).
- [38] F. Lyonnet, A. Kusina, T. Jeo, K. Kovak, F. Olness, *et al.*, “On the intrinsic bottom content of the nucleon and its impact on heavy new physics at the LHC,” [arXiv:1504.05156 \[hep-ph\]](#).
- [39] L. Massacrier, B. Trzeciak, F. Fleuret, C. Hadjidakis, D. Kikola, *et al.*, “Feasibility studies for quarkonium production at a fixed-target experiment using the LHC proton and lead beams (AFTER@LHC),” [arXiv:1504.05145 \[hep-ex\]](#).
- [40] E. Uggerhoj and U. I. Uggerhj, “Strong crystalline fields: A possibility for extraction from the LHC,” *Nucl.Instrum.Meth.* **B234** (2005) 31–39.
- [41] C. Barschel, “Precision luminosity measurement at LHCb with beam-gas imaging,”
- [42] M. Ferro-Luzzi, “Proposal for an absolute luminosity determination in colliding beam experiments using vertex detection of beam-gas interactions,” *Nucl.Instrum.Meth.* **A553** (2005) 388–399.
- [43] LHCb Collaboration, R. Aaij *et al.*, “Precision luminosity measurements at LHCb,” *JINST* **9** no. 12, (2014) P12005, [arXiv:1410.0149 \[hep-ex\]](#).
- [44] HERMES Collaboration, A. Airapetian *et al.*, “The HERMES polarized hydrogen and deuterium gas target in the HERA electron storage ring,” *Nucl.Instrum.Meth.* **A540** (2005) 68–101, [arXiv:physics/0408137 \[physics\]](#).
- [45] J. R. Gaunt and W. J. Stirling, “Double Parton Distributions Incorporating Perturbative QCD Evolution and Momentum and Quark Number Sum Rules,” *JHEP* **1003** (2010) 005, [arXiv:0910.4347 \[hep-ph\]](#).
- [46] PHENIX Collaboration, A. Adare *et al.*, “Ground and excited charmonium state production in  $p + p$  collisions at  $\sqrt{s} = 200$  GeV,” *Phys.Rev.* **D85** (2012) 092004, [arXiv:1105.1966 \[hep-ex\]](#).
- [47] CDF Collaboration, D. Acosta *et al.*, “ $\Upsilon$  production and polarization in  $p\bar{p}$  collisions at  $\sqrt{s} = 1.8$ -TeV,” *Phys.Rev.Lett.* **88** (2002) 161802.
- [48] ATLAS Collaboration, G. Aad *et al.*, “Measurement of Upsilon production in 7 TeV pp collisions at ATLAS,” *Phys.Rev.* **D87** no. 5, (2013) 052004, [arXiv:1211.7255 \[hep-ex\]](#).
- [49] CMS Collaboration, S. Chatrchyan *et al.*, “Measurement of the  $\Upsilon(1S)$ ,  $\Upsilon(2S)$ , and  $\Upsilon(3S)$  cross sections in pp collisions at  $\sqrt{s} = 7$  TeV,” *Phys.Lett.* **B727** (2013) 101–125, [arXiv:1303.5900 \[hep-ex\]](#).
- [50] LHCb Collaboration, R. Aaij *et al.*, “Measurement of Upsilon production in pp collisions at  $\sqrt{s} = 7$  TeV,” *Eur.Phys.J.* **C72** (2012) 2025, [arXiv:1202.6579 \[hep-ex\]](#).
- [51] LHCb Collaboration, R. Aaij *et al.*, “Production of  $J/\psi$  and  $\Upsilon$  mesons in  $pp$  collisions at  $\sqrt{s} = 8$  TeV,” *JHEP*

- [1306](#) (2013) 064, [arXiv:1304.6977](#) [hep-ex].
- [52] H.-S. Shao, “HELAC-Onia: An automatic matrix element generator for heavy quarkonium physics,” *Comput.Phys.Commun.* **184** (2013) 2562–2570, [arXiv:1212.5293](#) [hep-ph].
- [53] A. Martin, W. Stirling, R. Thorne, and G. Watt, “Parton distributions for the LHC,” *Eur.Phys.J.* **C63** (2009) 189–285, [arXiv:0901.0002](#) [hep-ph].
- [54] M. Whalley, D. Bourilkov, and R. Group, “The Les Houches accord PDFs (LHAPDF) and LHAGLUE,” [arXiv:hep-ph/0508110](#) [hep-ph].
- [55] **Particle Data Group** Collaboration, K. Olive *et al.*, “Review of Particle Physics,” *Chin.Phys.* **C38** (2014) 090001.
- [56] E. J. Eichten and C. Quigg, “Quarkonium wave functions at the origin,” *Phys.Rev.* **D52** (1995) 1726–1728, [arXiv:hep-ph/9503356](#) [hep-ph].
- [57] W. Buchmuller and S. Tye, “Quarkonia and Quantum Chromodynamics,” *Phys.Rev.* **D24** (1981) 132.
- [58] E. Braaten, B. A. Kniehl, and J. Lee, “Polarization of prompt  $J/\psi$  at the Tevatron,” *Phys.Rev.* **D62** (2000) 094005, [arXiv:hep-ph/9911436](#) [hep-ph].
- [59] E. Braaten, S. Fleming, and A. K. Leibovich, “NRQCD analysis of bottomonium production at the Tevatron,” *Phys.Rev.* **D63** (2001) 094006, [arXiv:hep-ph/0008091](#) [hep-ph].
- [60] M. Kramer, “Quarkonium production at high-energy colliders,” *Prog.Part.Nucl.Phys.* **47** (2001) 141–201, [arXiv:hep-ph/0106120](#) [hep-ph].
- [61] J. Pumplin, D. Stump, J. Huston, H. Lai, P. M. Nadolsky, *et al.*, “New generation of parton distributions with uncertainties from global QCD analysis,” *JHEP* **0207** (2002) 012, [arXiv:hep-ph/0201195](#) [hep-ph].
- [62] G. T. Bodwin, E. Braaten, and G. P. Lepage, “Rigorous QCD analysis of inclusive annihilation and production of heavy quarkonium,” *Phys.Rev.* **D51** (1995) 1125–1171, [arXiv:hep-ph/9407339](#) [hep-ph].